Feature Article: While theoretical and experimental efforts have thoroughly addressed microphase-ordered AB diblock copolymer blends with a parent homopolymer (hA or hB) or a second block copolymer, surprisingly few studies have considered comparable ABA triblock copolymers in the presence of hB or an AB diblock copolymer. In this study, we elucidate the roles of additive molecular weight *and* constraint by examining three matched series of miscible ABA/hB and ABA/AB blends. Self-consistent field theory is employed to analyze molecular characteristics, e.g., segmental distributions, microdomain periods and midblock bridging fractions, as functions of blend composition. Predictions are compared to morphological characteristics discerned by transmission electron microscopy and small-angle X-ray scattering. The corresponding mechanical properties of these blends are measured by dynamic mechanical analysis. The results of this comprehensive work reveal that addition of hB swells the B-lamellae of the ABA copolymer and has a generally deleterious effect on both the dynamic elastic modulus and midblock bridging fraction. In contrast, addition of a lamellar or cylindrical AB copolymer to the same ABA copolymer can promote an increase or decrease in lamellar period and bridging fraction, depending on relative block sizes.

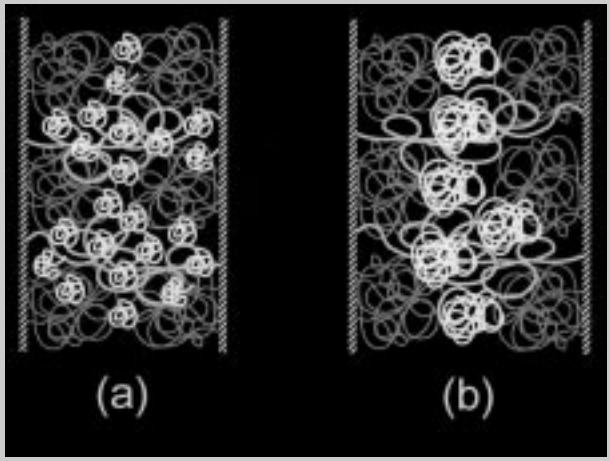

Schematic illustration of the B lamellae in a microphase-ordered ABA triblock copolymer physically blended with a B-selective homopolymer. The added B chains, identified by thick lines, are short relative to the B-midblock of the ABA copolymer in (a), but long in (b). Midblock bridges and loops appear as gray lines. Note the positional constraints placed on each species.

Molecular, Nanostructural and Mechanical Characteristics of Lamellar Triblock Copolymer Blends: Effects of Molecular Weight and Constraint

Lisaleigh Kane,[1] *David A. Norman,*[1a] *Scott A. White,*[2] *Mark W. Matsen,*[3] *Michael M. Satkowski,*[4] *Steven D. Smith,*[4] *Richard J. Spontak**[1]

[1] Departments of Materials Science & Engineering and Chemical Engineering, North Carolina State University, Raleigh, NC 27695, U.S.A.
[2] Medical Device Technologies Department, Becton Dickinson Technologies, Research Triangle Park, NC 27709, U.S.A.
[3] Polymer Science Centre, University of Reading, Whiteknights, Reading RG6 6AF, United Kingdom
[4] Corporate Research Division, The Procter & Gamble Company, Cincinnati, OH 45239, U.S.A.

Introduction

Block copolymers are macromolecules composed of two or more different homopolymers that are chemically connected through covalent linkages. Due to the presence of such linkages, these macromolecules are capable of spontaneously ordering into periodic nanostructures if the constituent sequences are sufficiently incompatible.[1–5] Nanostructural elements result due to competition between repulsive interactions (enthalpic) and chain packing (entropic), and are sensitive to molecular design parameters such as monomer incompatibility, molecular weight, monomer asymmetry and composition. Equilibrium nanostructures established[6] to date in neat block copolymers include spheres of A(B) arranged on a body-centered cubic lattice in a B(A) matrix, cylinders of A(B) arranged on a hexagonal lattice in a B(A) matrix, cubic bicontinuous channels and co-alternating lamellae. Long-lived metastable morphologies have also been

[a] Current address: Department of Materials Science & Engineering, University of Michigan, Ann Arbor, MI 48109, U.S.A.

  1022-1336/2001/0503–0281$17.50+.50/0

observed[7,8] in neat block copolymers. Unlike conventional polymer blends, which are prepared by physically mixing two or more polymer species in the molten[9–11] or solid state,[12,13] however, the composition of a block copolymer is typically varied through the chemical synthesis of new copolymer molecules. Attempts to overcome this limitation have demonstrated, experimentally and theoretically, that intermediate morphologies or nanostructures with specific dimensions can be reliably produced in miscible blends of an ordered diblock copolymer and a block-selective (parent) homopolymer[14–21] or a second block copolymer.[22–30]

Studies addressing such blends have, for the most part, employed AB diblock copolymers. Upon microphase ordering, the A and B blocks of these macromolecules behave as polymer chains that are grafted at one end (as *tails*) to a repulsive surface and consequently form a dense brush.[31,32] In this regard, the AB diblock constitutes the simplest copolymer architecture. While the morphologies and properties of copolymers with more complex linear architectures have been investigated,[5,33–39] we turn our attention here to the ABA triblock design. As with AB diblock copolymers, ABA triblocks can microphase-order into the classical spherical, cylindrical and lamellar morphologies,[40–42] as well as the complex gyroid morphology.[43–45] The principal difference between the two architectures is the double-tethered nature of the B midblock in the triblock. Each midblock adopts either a bridged or looped conformation by depositing its ends (the block junction sites) in adjacent interphases or the same interphase, respectively. Bridged midblocks endow ABA copolymers with superior mechanical properties relative to their AB analogs by forming a physically crosslinked network. For this reason, several theoretical formalisms capable of rendering predictions for the bridging fraction (υ_b) in lamellar ABA copolymers have been proposed.[46–49] According to self-consistent field theory (SCFT), υ_b lies between 0.40 and 0.45 for copolymers of modest incompatibility.[36] These predictions are in excellent agreement with the experimental results of Watanabe and co-workers,[50–52] who have developed a dielectric relaxation method by which to measure υ_b. The bridging fraction has also been calculated by Matsen and Thompson[41] for other morphologies, but these predictions have yet to be tested.

In this study, we extend the strategy of producing designer polymer nanostructures through physical blending to ABA triblock copolymers. To do so, we concurrently examine and relate the molecular, morphological and mechanical properties of a lamellar ABA triblock copolymer in the presence of either a B-selective homopolymer or an AB diblock copolymer. Examples of such blends are depicted in Figure 1. Relevant molecular characteristics (e.g., υ_b and segmental density distributions) are predicted by SCFT, while morphological features are elucidated by transmission electron microscopy (TEM) and small-angle X-ray scattering (SAXS). Dynamic mechanical analysis (DMA) is performed to ascertain the effect of homopolymer or copolymer additive on midblock bridging and, hence, network formation.

Experimental Part

Materials

Four polystyrene-*block*-polyisoprene-*block*-polystyrene (SIS) triblock copolymers, three polystyrene-*block*-polyisoprene (SI) diblock copolymers and three polyisoprene homopolymers (hI) were synthesized via living anionic polymerization with *sec*-butyllithium in cyclohexane at 60 °C. Copolymer compositions were measured by ^{1}H NMR spectroscopy. Molecular weight characteristics, such as the number- and weight-average molecular weights ($\overline{M}_n$ and $\overline{M}_w$, respectively), were discerned from GPC using polystyrene standards. Polydispersity indices ($\overline{M}_w/\overline{M}_n$) were consistently less

Richard J. Spontak received his B.S. degree with high distinction and honors in Chemical Engineering from the Pennsylvania State University in 1983 and his Ph.D. in Chemical Engineering from the University of California at Berkeley in 1988. He then served as a post-doctoral research associate in Materials Science & Metallurgy at the University of Cambridge and as a research fellow in Physics at the Institutt for Energiteknikk in Norway prior to becoming a staff member in the Corporate Research Division of the Procter & Gamble Company. In 1992, he joined the faculty at North Carolina State University, where he is presently Associate Professor of Chemical Engineering and Materials Science & Engineering. His research focuses on the design, characterization and thermodynamics of novel multicomponent polymer systems, especially those exhibiting an element of molecular self-organization or produced by creative process strategies. He is the recipient of an Alcoa Foundation Research Achievement Award, a Sigma Xi Outstanding Research Achievement Award, an Alexander von Humboldt Research Fellowship and an Outstanding Teaching Award. He has published over 130 papers in refereed journals, and his work has been featured on 7 journal covers, including last year's edition of Macromolecular Materials and Engineering. He dedicates the present work to the memory of his recently deceased father.

Table 1. Molecular characteristics of the materials used in this study.

Designation	Architecture	Morphology[a)]	w_I[b)]	$\bar{M}_n$[c)]	M_I	M_S	R_I[d)]
SIS	triblock copolymer	Lam	0.46	111 000	51 000	30 000	–
hI8	homopolyisoprene	–	1.00	7 500	7 500	–	0.29
hI15	homopolyisoprene	–	1.00	15 000	15 000	–	0.59
hI30	homopolyisoprene	–	1.00	30 000	30 000	–	1.18
SI15	diblock copolymer	Lam	0.30	50 000	15 000	35 000	0.59
SI30	diblock copolymer	Lam	0.46	65 000	30 000	35 000	1.18
SI48	diblock copolymer	Cyl	0.64	75 000	48 000	27 000	1.88
SISa[e)]	triblock copolymer	Lam	0.40	100 000	40 000	30 000	–
SISb[e)]	triblock copolymer	Lam	0.55	133 000	73 000	30 000	–
SISc[e)]	triblock copolymer	Cyl	0.60	150 000	90 000	30 000	–

[a)] Ascertained by TEM observations.
[b)] Discerned by ^{1}H NMR spectroscopy.
[c)] Measured by GPC.
[d)] Determined from the ratio of M_I to 0.5 $M_I^{(SIS)}$.
[e)] Not used in the preparation of any blends.

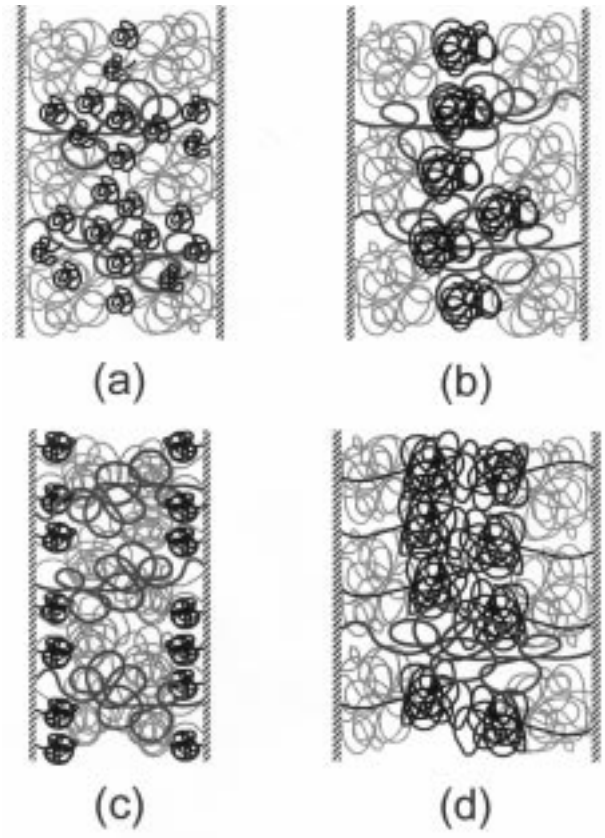

Figure 1. Schematic illustration of the B lamellae in a microphase-ordered ABA triblock copolymer physically blended with a B-selective homopolymer (a, b) or an AB diblock copolymer (c, d). The added B chains/blocks, identified by thick black lines, are short relative to the B-midblock of the ABA copolymer in (a, c), but long in (b, d). Midblock bridges and loops appear as black speckled and gray lines, respectively. Note the positional constraints placed on each species.

than 1.04. The material designation, mass fraction of I (w_I) and $\bar{M}_n$ of each material are provided in Table 1. Also included in Table 1 are the molecular weights of the I and S segments (M_I and M_S, respectively). Note that the value of M_S in all the block copolymers was relatively constant (ranging between 27 000 and 35 000), whereas M_I was systematically varied. Values of the I molecular weight ratio (R_I), defined as $2M_I/M_I^{(SIS)}$ (a factor of 2 is introduced to account for the biconformational nature of the midblock in the SIS copolymer), are provided for comparison in Table 1.

Methods

Films of the neat copolymers and blends of one SIS copolymer (see Table 1) with either hI or SI were prepared by first dissolving the requisite materials in toluene to form a 5% (w/v) solution. These solutions were cast into Teflon molds, and the solvent was removed slowly over the course of three weeks. Resultant films were then annealed under vacuum for 5 h at 110 °C to remove residual solvent, relax built-in stresses and promote nanostructural refinement. These films were cross-sectioned at −100 °C in a Reichert-Jung Ultracut-S cryoultramicrotome to obtain electron-transparent sections for TEM. The sections were subsequently exposed to the vapor of 2% OsO_4(aq) for 90 min to selectively stain the unsaturated bonds of the I repeat units. Images of the copolymers and the SIS blends were acquired with a Zeiss EM902 electron spectroscopic microscope operated at 80 kV and energy-loss settings (ΔE) between 50 and 120 eV. Small-angle X-ray scattering was performed on bulk films with CuK_α radiation (λ = 0.154 nm) from a Rigaku RU-300 rotating anode. The generator was operated at 40 kV and 200 mA, and data were acquired with Kratky optics. Resultant scattering patterns were not desmeared since the beam size was small relative to the sample-to-detector distance. One-dimensional patterns display scattered intensity (in arbitrary units) as a function of the scattering vector ($\boldsymbol{q}$), where $\boldsymbol{q} = (4\pi/\lambda)\sin(\theta/2)$ and θ denotes the scattering angle. Dynamic mechanical tests were conducted on specimens measuring 35 mm × 5 mm × 0.5 mm with a Rheometrics Solids Analyzer (RSAII) operated at 25 °C in tensile mode. Limited shear tests were also performed on molten specimens with a Rheometrics Mechanical Spectrometer (RMS800) at 150 °C using

parallel plates. The dynamic storage modulus (E' in tensile mode or G' in shear mode) was measured as a function of frequency (ω) at a strain amplitude of 0.01% in tensile mode or <5% in shear mode (all the strain amplitudes employed here have been examined to ensure that they lie within the linear viscoelastic regime). At least three specimens were subjected to testing to assure reproducibility.

Theory

The theoretical segmental density distributions and bridging statistics presented here are obtained from SCFT. The application of SCFT to block copolymer blends has been previously described,[20] and straightforward extension of this method yields the segmental distributions and self-consistent fields for the lamellar microphase of a triblock/homopolymer or triblock/diblock blend. Once these are obtained, the bridging statistics can be evaluated using the technique developed earlier.[36] This involves calculating the triblock junction distribution at a single interface, and then propagating that distribution along the middle block to the second junction site. The final distribution exhibits two peaks, one representing loops at the initial interface and another corresponding to bridges at the adjacent interface. The bridging fraction is subsequently determined by integrating the area under each peak. To determine the volume fractions required for the calculation, we use homopolymer (hS and hI) densities of 1.00 and 0.84 g/cm^3, respectively.[19] These densities yield 0.497 as the S volume fraction of the SIS triblock copolymer. Analogous S volume fractions for the SI15, SI30 and SI48 diblock copolymers are 0.662, 0.495 and 0.321, respectively, and the volumes of the SI copolymers relative to the SIS copolymer are 0.438, 0.586 and 0.697, respectively. The calculation also requires the conformational asymmetry between S and I segments. Using the chain dimensions reported[19] for hS and hI, we determine the ratio of the statistical segment lengths (on the basis of a common segment volume) to be 0.92. A reliable estimate of the Flory-Huggins interaction parameter (χ) is difficult to obtain, but fortunately the bridging statistics are not very sensitive to χ. From calculations presented elsewhere,[47] we elect to use χN = 80, where N denotes the degree of polymerization of the triblock.

Results and Discussion

Preliminary Considerations

Transmission electron micrographs of the three SI diblock copolymers used to prepare SIS/SI blends are presented in Figure 2 and reveal that the SI15 and SI30 copolymers (Figure 2a and 2b, respectively) exhibit the lamellar morphology. The lamellar nanostructure of the SIS copolymer is virtually identical to that of the SI30 and is not included here for that reason. In contrast, the SI48 copolymer (Figure 2c) consists of hexagonally-packed S cylinders embedded in an I matrix. As mentioned earlier, the I units appear electron-opaque (dark) in these images due to selective OsO_4 staining. Two of the other SIS copolymers synthesized during the course of this study, but not used in any of the blends, likewise exhibit lamellae, while one also possesses S cylinders (see Table 1). Only lamellar SIS/hI and SIS/SI blends, as verified by TEM and SAXS, are considered further in this work. Non-lamellar (possibly bicontinuous) morphologies have been observed[53] in some of the SIS/hI8 and SIS/SI48 blends.

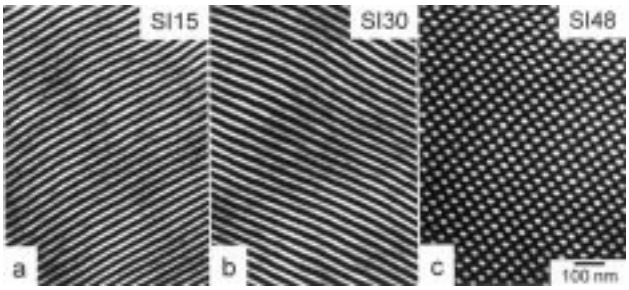

Figure 2. Transmission electron micrographs of the three SI diblock copolymers used in this study: (a) SI15, (b) SI30 and (c) SI48. The morphology of the SIS copolymer is identical to that of the SI30 copolymer and is not reproduced here. The molecular characteristics of all the copolymers employed here are provided in Table 1. As seen in this series of images, the B-lamellae in these microphase-ordered block copolymers are stained with OsO_4 and appear electron-opaque (dark).

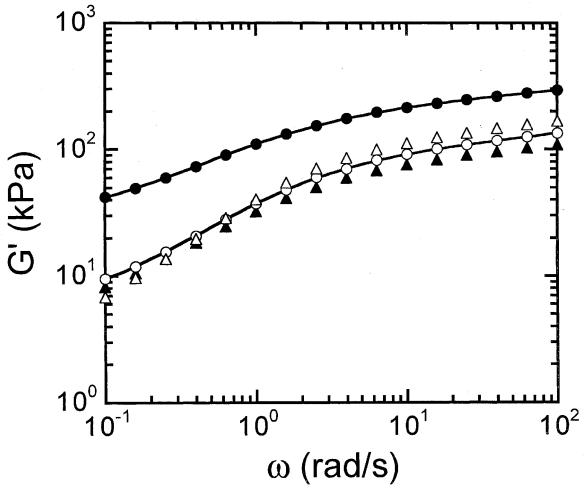

Figure 3. Frequency (ω) spectra of the dynamic elastic shear modulus (G') at 150 °C for the SIS copolymer before (●) and after (▲) being subjected to a strain of 106 strain units. Values of $G'(\omega)$ acquired for a SIS/SI30 blend (w_{SI} = 0.2) before (○) and after (△) exposure to a strain of 122 strain units at 150 °C are also displayed. The solid lines connect the data of the undeformed materials.

Figure 3 displays the ω spectrum of G' for the neat SIS copolymer and one of the SIS/SI30 blends (with a diblock mass fraction, w_{SI}, of 0.2) at 150 °C. In this figure, G' for both materials is seen to increase with increasing ω over

the range of ω examined. This feature is characteristic of all the lamellar block copolymer systems investigated in this work. The most significant difference between these two spectra in Figure 3 is the magnitude of G'; i.e., G'_{SIS} is more than 4 × greater than G'_{blend} at $\omega = 10^{-1}$ rad/s. As will be shown later, this SIS/SI30 blend possesses a value of E' that is comparable to that of the neat SI30 copolymer, suggesting that the SIS/SI30 blend and the SI30 copolymer possess similar block conformations (*loops* can be envisaged as *tails* of half molecular weight). It therefore seems reasonable to attribute the observed difference in G' between the SIS copolymer and the SIS/SI30 blend to a greater population of bridged midblocks in the neat copolymer. [Although interdigitated loops from adjacent interfaces should contribute to G' in the same fashion as bridges, their population is expected to closely track that of the bridges, and so we ignore them in the following qualitative discussions.[54]] To test this hypothesis, the ω spectra of the SIS copolymer and the SIS/SI30 blend are also examined after the materials are subjected to large strains. By doing so, we envisage that one end of each of the bridged midblocks present in both materials is pulled out so that these midblocks form either loops or dangling ends.[55]

Included in Figure 3 is the ω spectrum obtained from the SIS copolymer after being strained to 106 strain units. The entire spectrum appears to be shifted down to lower G' and coincides almost exactly with the original spectrum of the blend. After being subjected to a strain of 122 strain units, the ω spectrum of the blend does not perceivably change. These results are consistent with our hypothesis and, neglecting the possibility of orientation effects,[56] confirm that the magnitude of the dynamic storage modulus within the linear viscoelastic regime is sensitive to the population of bridged midblocks within SIS-containing systems. Values of G' for the SIS copolymer evaluated at $\omega = 10^{-1}$ rad/s before and after large-strain deformation are about 42.2 and 8.21 kPa. The post-strain value of G'_{SIS} is seen to be in reasonably good quantitative agreement with the pre- and post-strain values of G' for the SIS/SI30 blend (9.59 and 6.84 kPa, respectively). Throughout the remainder of this work, we use the magnitude of the low-ω dynamic storage modulus (at 10^{-1} rad/s) as a measure by which to compare, at least qualitatively, the mechanical properties (and, hence, the bridge fraction) of the SIS/hI and SIS/SI blend series. This methodology has been previously employed[53] to identify a transition from the lamellar to a bicontinuous morphology in the SIS/hI8 series.

Triblock Copolymer/Homopolymer Blends

Segmental Distributions

Predicted segmental distributions for I in a 50/50 v/v SIS/hI30 blend are displayed in Figure 4 and resemble analogous distributions provided elsewhere[20, 21] for diblock/homopolymer blends. Each I lamella consists of I segments deposited from the midblock of the SIS copolymer, as well as from hI. The stretched I blocks of the copolymer tend to push the hI molecules towards the center of the I lamellae, as confirmed by Lee et al.[57] in their small-angle neutron scattering (SANS) studies of triblock copolymer/homopolymer blends. Such confinement is countered by the translational entropy of the homopolymer, which favors a uniform distribution within the lamellae. Since the translational entropy is proportional to the number concentration of homopolymer molecules, its effect increases as the homopolymer molecular weight decreases. Thus, an increase in M_{hI} promotes sharper segmental distributions of I from both the copolymer midblock and hI, whereas a reduction in M_{hI} is conversely accompanied by broader distributions. These two scenarios are schematically depicted in Figure 1a and 1b, respectively, and suggest that M_{hI} influences the extent to which the copolymer midblocks are capable of forming bridges. If, for example, M_{hI} is relatively large, a midblock may be unable to traverse the span of its lamella and form a bridge, in which case more loops form. Another issue regarding M_{hI} is that, as M_{hI} decreases and hI molecules become increasingly more evenly distributed, the hI molecules will progressively wet the layers of midblock loops and eventually affect interfacial chain packing and, ultimately, interfacial curvature.[58] This possibility is not, however, pursued further in this work, since only lamellar blends are explicitly considered. While the segmental distributions of I depend on M_{hI} and hI concentration, the one presented in Figure 4 provides a general picture of such distributions in lamellar SIS/hI blends.

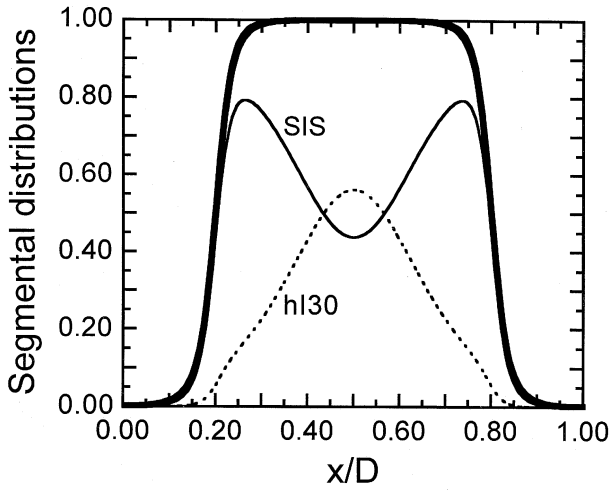

Figure 4. Segmental distribution of I (thick line) presented as a function of distance (normalized with respect to the lamellar period, D) for a 50/50 v/v blend of the SIS copolymer and hI30 homopolymer examined in this study. The distributions of I segments deposited from the copolymer and homopolymer (solid and dashed thin lines, respectively) are also shown.

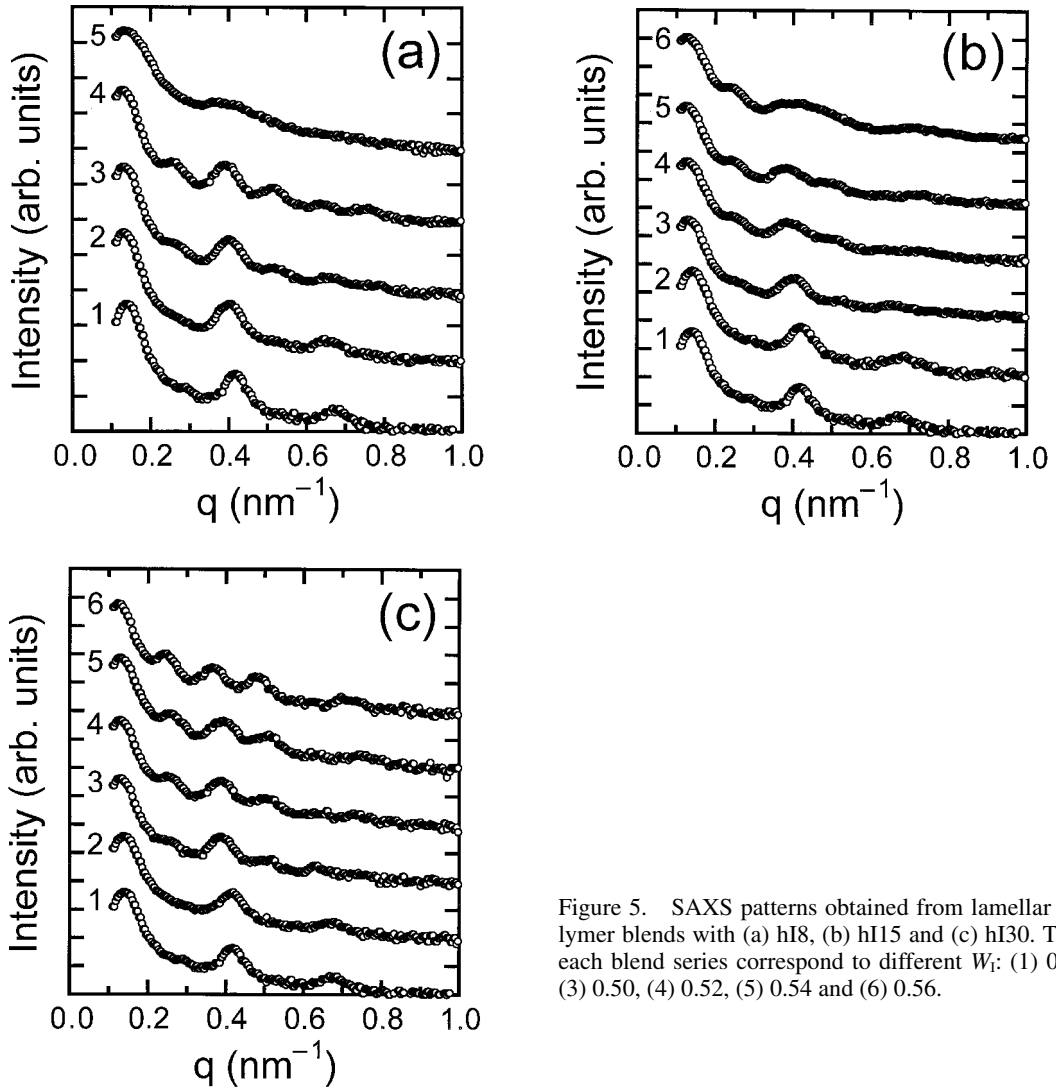

Figure 5. SAXS patterns obtained from lamellar SIS/homopolymer blends with (a) hI8, (b) hI15 and (c) hI30. The profiles in each blend series correspond to different W_I: (1) 0.46, (2) 0.48, (3) 0.50, (4) 0.52, (5) 0.54 and (6) 0.56.

Morphological Features

Small-angle X-ray scattering patterns are shown in Figure 5 for the SIS blend series with hI8 (Figure 5a), hI15 (Figure 5b) and hI30 (Figure 5c). The SAXS pattern obtained from the neat SIS copolymer, in particular, exhibits regularly spaced peaks positioned at odd integral ratios relative to the principal peak. This observation is consistent with a lamellar nanostructure in which the alternating S and I lamellae are comparable in thickness. Recall that the volume fraction of S in the neat SIS copolymer is estimated to be 0.497. As hI is added to the copolymer, two trends become immediately evident from the data displayed in Figure 5. The first is that the position of each scattering peak tends to shift to lower $\boldsymbol{q}$. According to the inverse relationship between real and reciprocal space, this shift translates into an increase in lamellar thickness. Thus, addition of hI serves to swell the I lamellae of the SIS copolymer. The second trend apparent in this figure is that peaks corresponding to even integral peak ratios (relative to the principal peak) emerge and become increasingly more prominent as the concentration of hI increases in all three blend series.

Values of the lamellar period (D) extracted from the SAXS patterns shown in Figure 5 are presented as a function of blend composition (expressed as the total I mass fraction, W_I) in Figure 6. According to Bragg's law, D is given by $2\pi/\boldsymbol{q}^*$, where $\boldsymbol{q}^*$ denotes the position of the first-order (principal) scattering peak. Additional peaks have also been used whenever possible to ascertain D from Bragg's law appropriately generalized to include the peak order. The values of D evident in Figure 6 generally appear to increase with increasing W_I, which is consistent with lamellar swelling. As anticipated from the previous discussion, incorporation of hI30 molecules into the I lamellae of the SIS copolymer induces the most pronounced swelling. It must be recognized, however, that differences in these swelling data due to changes in M_{hI} are minimal, often within experimental uncertainty. An

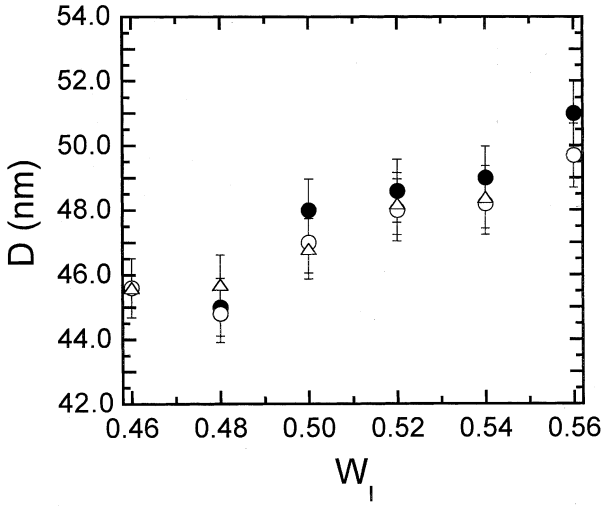

Figure 6. Lamellar period (D) discerned from SAXS and presented as a function of blend composition (W_I) for SIS/hI blends composed of hI8 (△), hI15 (○) and hI30 (●).

interesting feature of these data is that, at low concentrations of hI, D decreases slightly before it increases due to conventional swelling. This anomaly has been previously observed in diblock[14] and triblock[57] copolymer/homopolymer blends and, more noticeably, in a blend composed of a triblock copolymer and a midblock-selective solvent.[59] Since the density of the I lamellae must remain constant, one explanation for such lamellar contraction upon hI addition is that the hI molecules initially force the loops apart along the interfaces to which they are anchored so that the hI molecules can interdigitate within the loops. In this case, the copolymer nanostructure initially swells parallel to the lamellae, causing minor contraction along the lamellar normal.

Mechanical Properties

Frequency spectra of E' for the SIS/hI blend series are provided in Figure 7. As seen previously in Figure 3 with regard to $G'(\omega)$, values of E' are observed to increase monotonically with increasing ω in all the SIS/hI8 blends (Figure 7a). In addition, the shapes of the $E'(\omega)$ curves remain similar from $W_I = 0.46$ to $W_I = 0.52$. The data corresponding to $W_I = 0.54$ are, however, considerably less dependent on ω, which is consistent with a bicontinuous morphology such as the gyroid.[60] While TEM analysis of this blend reveals the existence of a lamellar morphology, the SAXS pattern in Figure 5a is inconclusive. Moreover, the blend with $W_I = 0.56$ clearly exhibits a non-lamellar (bicontinuous) morphology.[53] We therefore speculate that the blend with $W_I = 0.54$ lies sufficiently close to a microphase transition that it may contain elements of a bicontinuous nanostructure, which endow the blend with greater solid-like (less ω-dependent) character. Comparison of the ω spectra for the SIS/hI15 and

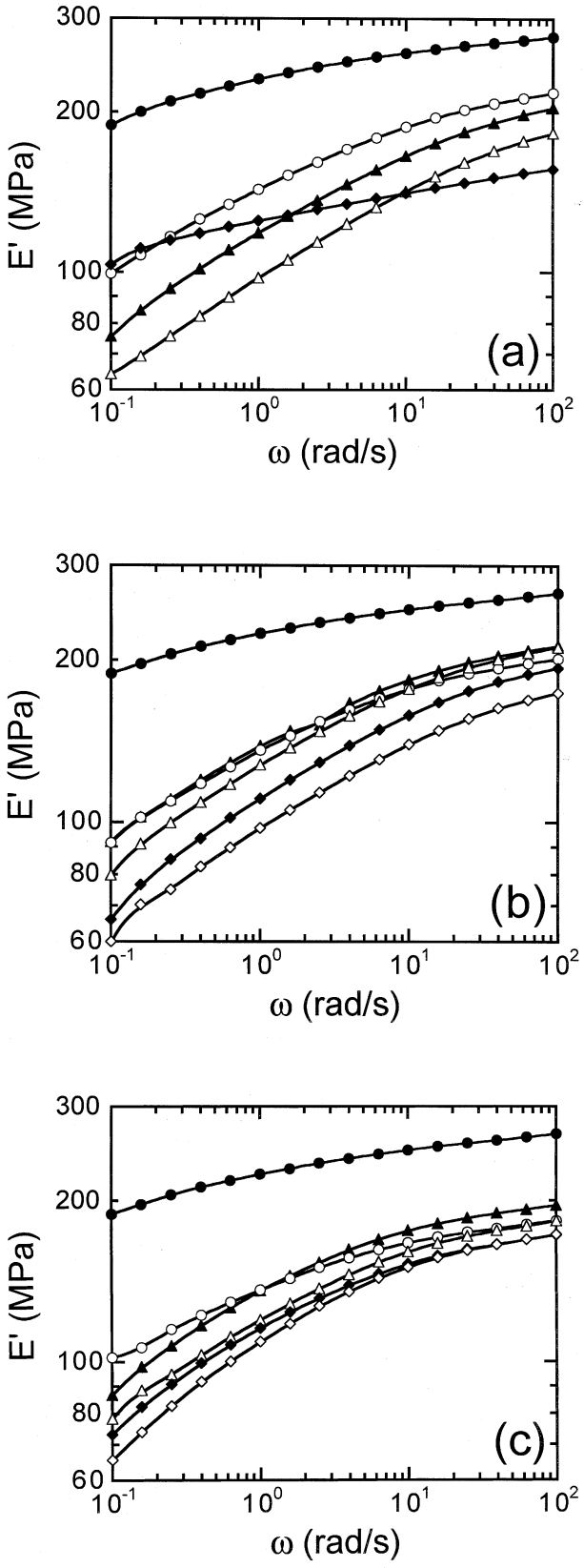

Figure 7. Dependence of the dynamic elastic tensile modulus (E') on ω for SIS/hI blends composed of (a) hI8, (b) hI15 and (c) hI30. In each series, W_I is varied: 0.46 (●), 0.48 (○), 0.50 (▲), 0.52 (△) and 0.54 (♦). The solid lines serve to connect the data.

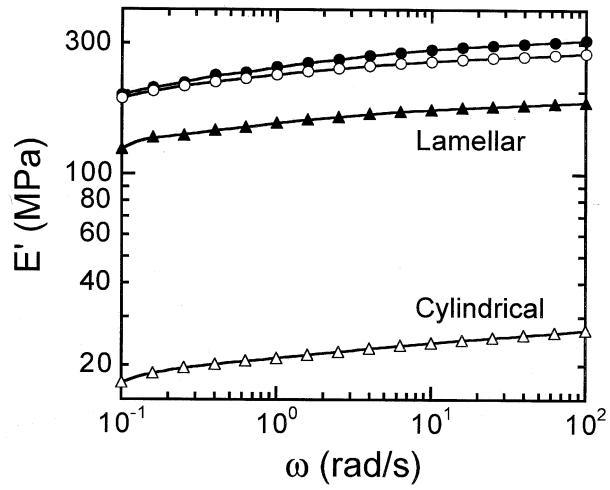

Figure 8. Frequency spectra of E' for neat SIS copolymers differing only in midblock mass: 40000 (●), 51000 (○), 73000 (▲) and 90000 (△). The molecular characteristics of these copolymers are provided in Table 1.

SIS/hI30 blend series in Figure 7b and 7c, respectively, reveals that none of the blends in either series shows any evidence of such a transition, confirming that all these blends are most likely lamellar (in agreement with TEM and SAXS analyses). Preservation of the lamellar morphology at higher hI concentrations is attributed to the increase in M_{hI} and the greater tendency for the hI molecules to reside near the lamellar midplane, away from the interfaces.[58] Analogous ω spectra acquired from the neat triblock copolymers (see Table 1) are shown in Figure 8 and demonstrate that E' decreases abruptly (by more than a factor of 7 at $\omega = 10^{-1}$ rad/s) and remains similarly ω-dependent upon going from the lamellar morphology to the cylindrical morphology.

Values of E' evaluated at $\omega = 10^{-1}$ rad/s from each of the curves displayed in Figure 7 and normalized with respect to E' of the neat SIS copolymer (hereafter designated E_0) are presented as a function of W_I in Figure 9a. Although the effect of M_{hI} on E' cannot be elucidated from the data displayed in this figure, it is apparent that, upon addition of hI, E'/E_0 decreases precipitously from 1.00 to about 0.55 or less, depending slightly on M_{hI}, as W_I is increased from 0.46 to 0.48. If we interpret these data in the same manner as those provided earlier in Figure 3, this reduction implies that incorporation of hI molecules into the I lamellae of the SIS copolymer effectively disrupts the ability of the midblocks to form bridges. [It should be recognized, however, that the elasticity of loops and bridges can be comparable if the bridges are not mutually entangled.[61]] Shown for comparison in Figure 9a is the value of E'/E_0 (=0.54) for the SI30 copolymer, which approximates the diblock analog (half molecular weight) of the SIS copolymer. Note that the SIS/hI blends evaluated at $W_I = 0.48$ exhibit almost identical

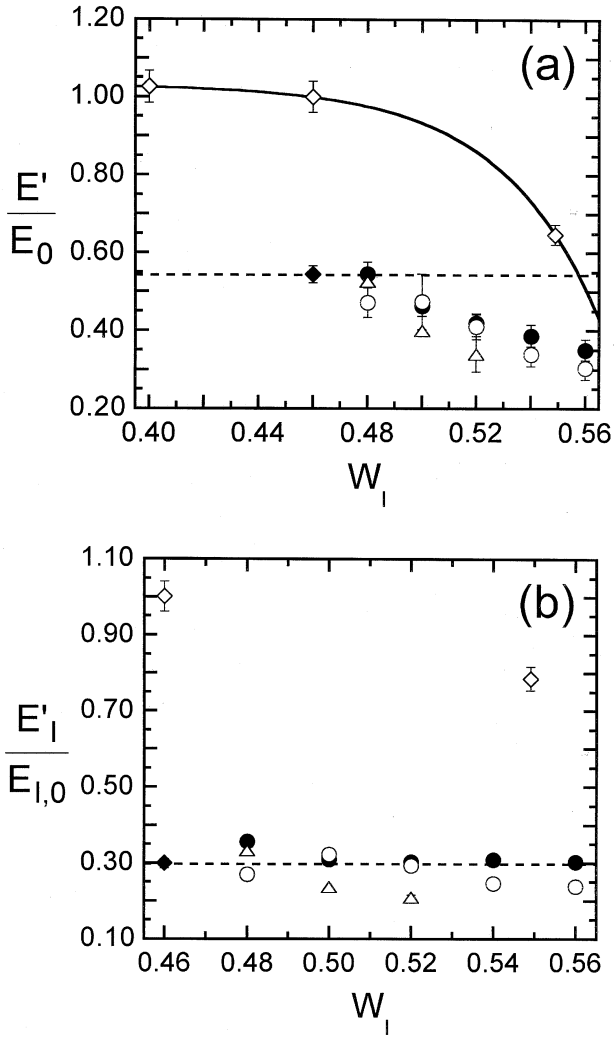

Figure 9. In (a), variation of E' evaluated at $\omega = 10^{-1}$ rad/s and normalized with respect to E_0 (E' of the SIS copolymer at the same ω) with respect to W_I for lamellar SIS/hI blends with hI8 (△), hI15 (○) and hI30 (●). Also shown are modulus ratios for the SI30 copolymer (♦) and two SIS copolymers (◇) not used in any blends. The solid line serves as a guide for the eye. Corresponding values of $E'_I/E_{I,0}$ derived from the GM model (Equation (2) in the text) are provided as a function of W_I in (b). The dashed line in each figure identifies the modulus ratio for the SI30 copolymer.

E'/E_0. As W_I is increased further, the values of E'/E_0 for the SIS/hI blends decrease further due to greater rubber-induced flexibility. Such enhanced flexibility is not, however, solely responsible for the initial reduction in E'/E_0 for the SIS/hI blends. Included in Figure 9a are E'/E_0 acquired from the neat SIS copolymers (see Figure 8). In this series, only the molecular weight of the I midblock (and, hence, molecular composition) is varied. According to SCFT predictions,[47] the bridging fraction (υ_b) is not anticipated to change much with composition within the lamellar microphase, in which case this triblock series provides a direct measure of how much E' is affected by rubber content alone. While E'/E_0 decreases from 1.00 to

about 0.65 as W_I is increased from 0.46 to 0.55, the increase in rubber content in this triblock series does not elicit the same mechanical response as in the SIS/hI blends. Thus, the data in Figure 9a indicate that the initial reduction in E'/E_0 for the SIS/hI blends reflects, at least in part, a decrease in υ_b.

On the basis of surface energy considerations, the specimen films prepared in this work are expected to consist of alternating bilayers that tend to orient parallel to the film surface, in which case the values of E' reported for the copolymers and copolymer/homopolymer blends in Figure 7 and 8 reflect contributions from both the S-rich glassy and I-rich rubbery lamellae. Prior attempts to decouple such contributions in highly oriented semicrystalline polymers have resulted in the series and parallel models proposed by Takayanagi et al.[62] Since tensile stress is applied along the lamellar normal in the measurements conducted here and since only the dynamic elastic modulus of the I-rich lamellae (E'_I) should be composition-dependent, it follows that the parallel Takayanagi model[63] would be applicable in the present analysis. This model can be written in terms of E'_I as

$$E'_I = (E' - \phi_S E'_S)/\phi_I \quad (1)$$

where ϕ_S and ϕ_I denote the volume fractions of the S- and I-rich lamellae, respectively, and E'_S is the tensile modulus of hS at ambient temperature. The value of E'_S is measured to be 1.00 ± 0.05 GPa over the ω range 0.1–1.0 rad/s for hS ($\overline{M}_n$ = 100000). [Within the glassy state, the tensile modulus is not very sensitive to molecular weight.[64]] In the absence of shear during microphase separation,[65] however, the lamellae most likely do not exhibit global orientation due to the presence of defects and grains that develop as the block copolymer molecules microphase-separate. For unoriented composite polymers, Gray and McCrum[66] suggest a logarithmic mixing rule given by

$$\log E'_I = (\log E' - \phi_S \log E'_S)/\phi_I \quad (2)$$

Since the degree of lamellar orientation in the specimens examined here is not known, we elect to use the Gray-McCrum (GM) model to extract E'_I from the data provided in Figure 7 and 8. The composition dependence of $E'_I/E_{I,0}$ evaluated at $\omega = 10^{-1}$ rad/s is shown for comparison in Figure 9b and clearly reveals that $E'_I/E_{I,0}$ decreases with increasing W_I for the neat SIS copolymers, but is surprisingly insensitive to both M_{hI} and W_I for the SIS/hI blends and the SI30 diblock copolymer.

Molecular Characteristics

To discern the role of the hI molecules in the development of blend morphology and properties, we now examine the molecular characteristics of the SIS/hI blends discussed thus far. Predictions for D, normalized with respect to the unperturbed end-to-end distance of the neat SIS copolymer, are presented as a function of blend composition in Figure 10. In this case, composition is expressed in terms of the homopolymer volume fraction (ϕ_{hI}). Comparison of experimental D values in Figure 6 with theoretical D values in Figure 10 reveals good qualitative agreement in that D generally increases (i.e., the lamellae swell) with increasing hI content. Further comparison is possible by recognizing that W_I = 0.56 corresponds to ϕ_{hI} = 0.21, in which case the range of data shown in Figure 6 corresponds to about 2/3 of the abscissa displayed in Figure 10. Predicted, as well as experimental, values of D do not vary substantially with M_{hI} over this composition range. According to SCFT predictions and intuitive expectation, hI30 should consistently promote the greatest degree of lamellar swelling in the SIS copolymer.

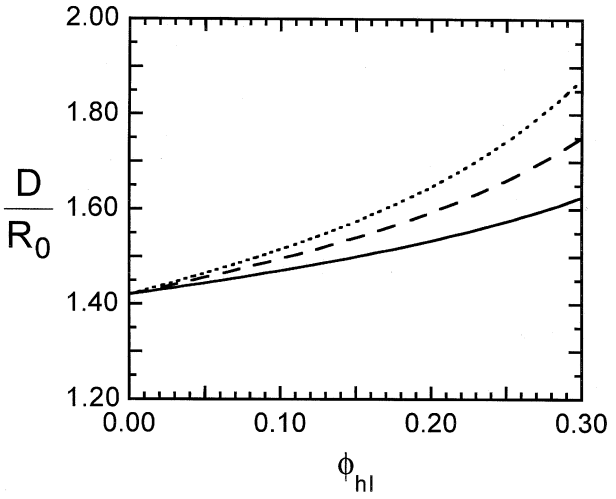

Figure 10. Predicted D normalized with respect to the unperturbed end-to-end distance of the neat SIS copolymer (R_0) and presented as a function of homopolymer concentration (ϕ_{hI}) for the SIS/hI blend series with hI8 (solid line), hI15 (dashed line) and hI30 (dotted line).

Figure 11 shows predicted υ_b as a function of hI concentration in each of the SIS/hI blends examined here. For the neat SIS copolymer, the theory predicts that 44% of the SIS molecules will form bridges, which is in excellent agreement with dielectric relaxation measurements.[50–52] Note that υ_b in the lamellar morphology cannot exceed 50% if the chains are flexible.[36] As seen in this figure, incorporation of hI30 into the lamellar SIS matrix is predicted to promote the greatest reduction in υ_b (from 0.44 at ϕ_{hI} = 0.0 to 0.29 at ϕ_{hI} = 0.2). This result confirms that, as M_{hI} is increased for a given blend composition, hI molecules increasingly inhibit the formation of midblock bridges by occupying the midplane region of each I lamella. For a given M_{hI}, υ_b is likewise predicted to

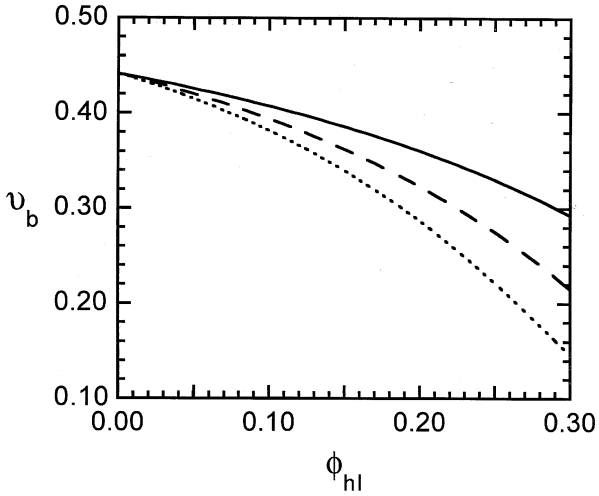

Figure 11. SCFT predictions of the midblock bridging fraction (υ_b) as a function of ϕ_{hI} for the same blend series described in the caption of Figure 10.

decrease with increasing hI concentration due to a greater population of hI molecules residing along the lamellar midplane. In either case, as υ_b decreases, the difference in mechanical properties between a triblock and its diblock analog lessens, eventually becoming negligible (recall that loops are expected to possess comparable mechanical properties as tails). These predictions for υ_b are therefore generally consistent with the DMA results presented in Figure 9.

Triblock/Diblock Copolymer Blends

Segmental Distributions

In this section, we examine analogous molecular, morphological and property issues in lamellar SIS/SI blends as in the previous SIS/hI blends. It is important to recognize that, unlike the hI molecules employed earlier, the I blocks of the SI copolymers are each physically anchored at one end (the junction site), which serves to constrain these blocks more relative to their hI analogs. This molecular constraint has a generally profound effect on the packing of the I midblocks deposited by the SIS copolymer. Segmental distributions predicted by SCFT for each of the SIS/SI blends investigated here are presented in Figure 12 and reveal that M_I of the SI diblock strongly influences the spatial arrangement of chains within each I lamella. If, on one hand, the SI copolymer possesses a relatively short I block, as in the case of SI15 (Figure 12a), the I blocks from the SI copolymer fill space close to the interface, as illustrated in Figure 1c. Such block arrangement forms a bidisperse polymer layer,[28, 67–69] forcing the I blocks from the SIS copolymer to reside near the lamellar midplane and promoting the formation of midblock bridges.

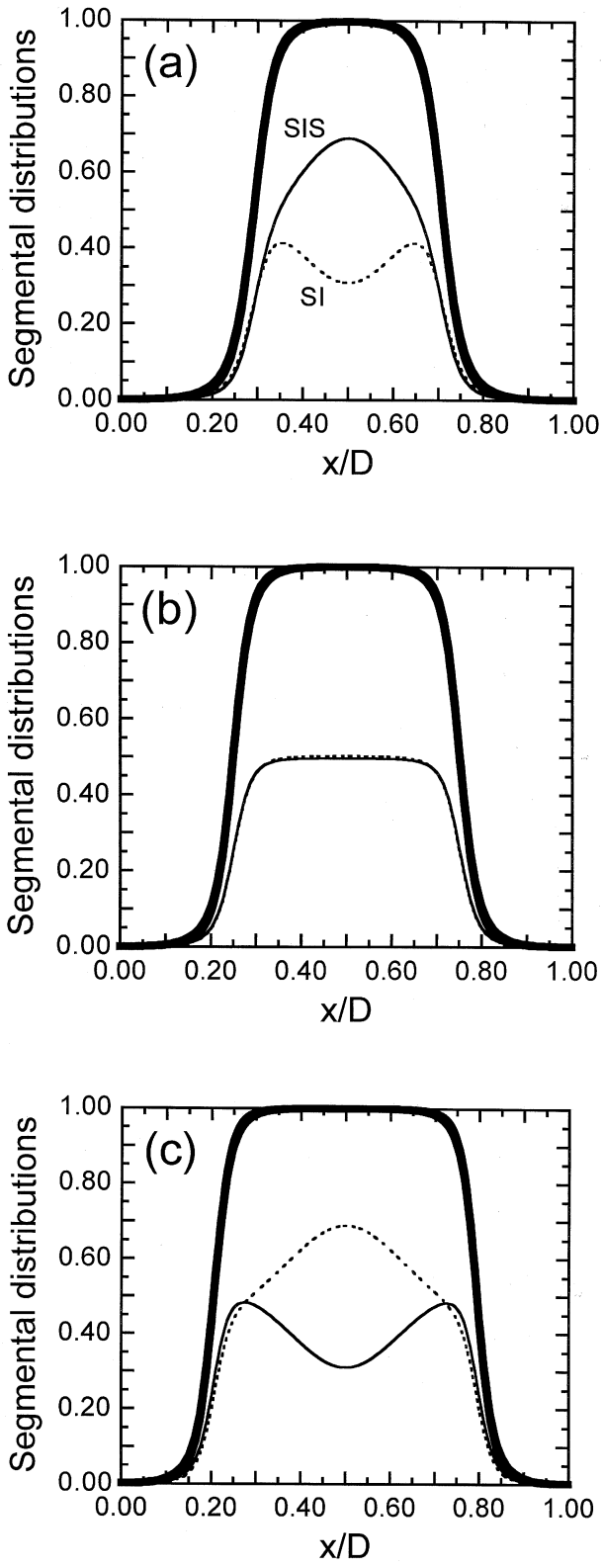

Figure 12. Segmental distribution of I (thick line) presented as a function of normalized distance for miscible 50/50 v/v blends of the SIS copolymer and either (a) SI15, (b) SI30 or (c) SI48. The distributions of I segments deposited from the triblock and diblock (solid and dashed thin lines, respectively) are also shown.

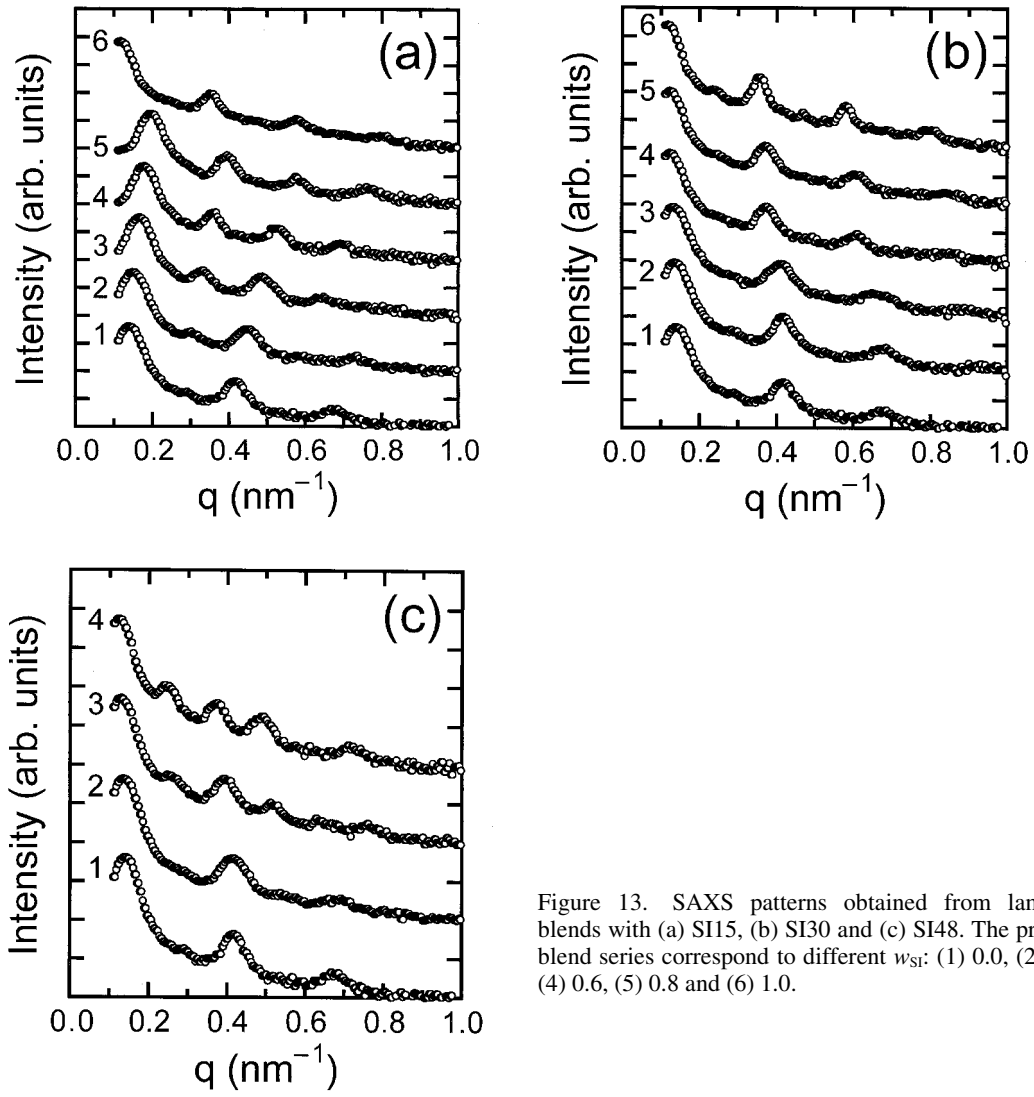

Figure 13. SAXS patterns obtained from lamellar SIS/SI blends with (a) SI15, (b) SI30 and (c) SI48. The profiles in each blend series correspond to different w_{SI}: (1) 0.0, (2) 0.2, (3) 0.4, (4) 0.6, (5) 0.8 and (6) 1.0.

Diblock molecules with long I blocks, on the other hand, have the opposite effect. According to the SCFT predictions provided in Figure 12c and the illustration shown in Figure 1d, the I blocks of the SIS copolymer must occupy space near the interface, while those of the SI copolymer locate primarily along the lamellar midplane to ensure uniform volume filling. In this case, as with large hI molecules, the bridging fraction is expected to decrease significantly due to obstructed bridge formation. Another important consideration regarding molecular arrangement, as well as morphological and property development, is how the SI molecules affect the width of the I lamellae. As the I lamellae become narrower, bridge formation becomes more probable for a given SIS copolymer. Generally speaking, SIS/SI blends composed of SI molecules with relatively short I blocks tend to reduce the thickness of the I lamellae. Thus, the block stratification and lamellar thinning that simultaneously occur in such blends favor the formation of midblock bridges and a corresponding increase in the bridging fraction (υ_b). We return to discuss this point later.

Morphological Features

Small-angle X-ray scattering patterns acquired from each of the SIS/SI blend series are shown in Figure 13. According to the data displayed in Figure 13a, an increase in the concentration of the SI15 copolymer in the SIS/SI15 blend series is accompanied by a shift of the scattering peaks to larger $\boldsymbol{q}$, which indicates that the I lamellae become increasingly thinner (recall from Table 1 that the S blocks of the SI and SIS copolymers are of comparable molecular weight). A gradual shift in peak position with changing blend composition provides evidence that the blends are miscible, i.e., a single nanostructure forms. (Phase separation in block copolymer

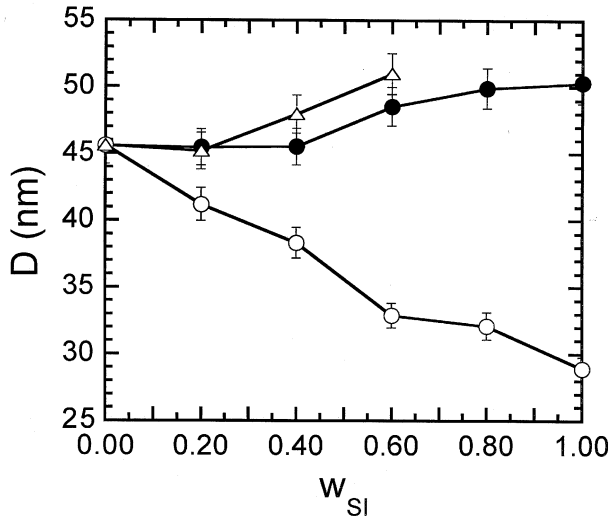

Figure 14. Lamellar period (D) discerned from SAXS and presented as a function of blend composition (w_{SI}) for SIS/SI blends composed of SI15 (○), SI30 (●) and SI48 (△). The solid lines serve to connect the data.

blends is readily detected by the existence of two superimposed scattering patterns.[26, 70]) Complete miscibility of these blends is expected[29] on the basis of the R_I values provided in Table 1 ($R_I < 1.9$) and is confirmed by TEM. The SAXS patterns obtained from the SIS/SI30 (Figure 13b) and SIS/SI48 (Figure 13c) blends reveal that an increase in SI content promotes a shift of the scattering peaks to smaller $\boldsymbol{q}$ and, hence, lamellar swelling. Note that, since the SI48 copolymer consists of hexagonally-arranged S cylinders in an I matrix (see Figure 2c), some of the SIS/SI48 blends produced here are non-lamellar. Only those that exhibit the lamellar morphology are considered further. Values of D extracted from the SAXS data provided in Figure 13 are presented as a function of blend composition (expressed in terms of the mass fraction of the SI copolymer, w_{SI}, in the blend) in Figure 14. As inferred from the SAXS patterns, D increases non-linearly with increasing w_{SI} for blends containing the SI30 and SI48 copolymers, but decreases with increasing w_{SI} for blends with the SI15 copolymer.

Mechanical Properties

Frequency spectra of the SIS/SI blends are displayed for comparison in Figure 15. These $E'(\omega)$ data closely resemble those shown earlier for the SIS/hI blends (see Figure 7) and indicate that all the SIS/SI15 and SIS/SI30 blends (Figure 15a and 15b, respectively) exhibit comparable mechanical responses and, by inference, the lamellar morphology (in agreement with SAXS and TEM observations). In contrast, E' is less dependent on ω in the SIS/SI48 blend with w_{SI} = 0.8 (Figure 15c) and is most likely non-lamellar. According to complementary

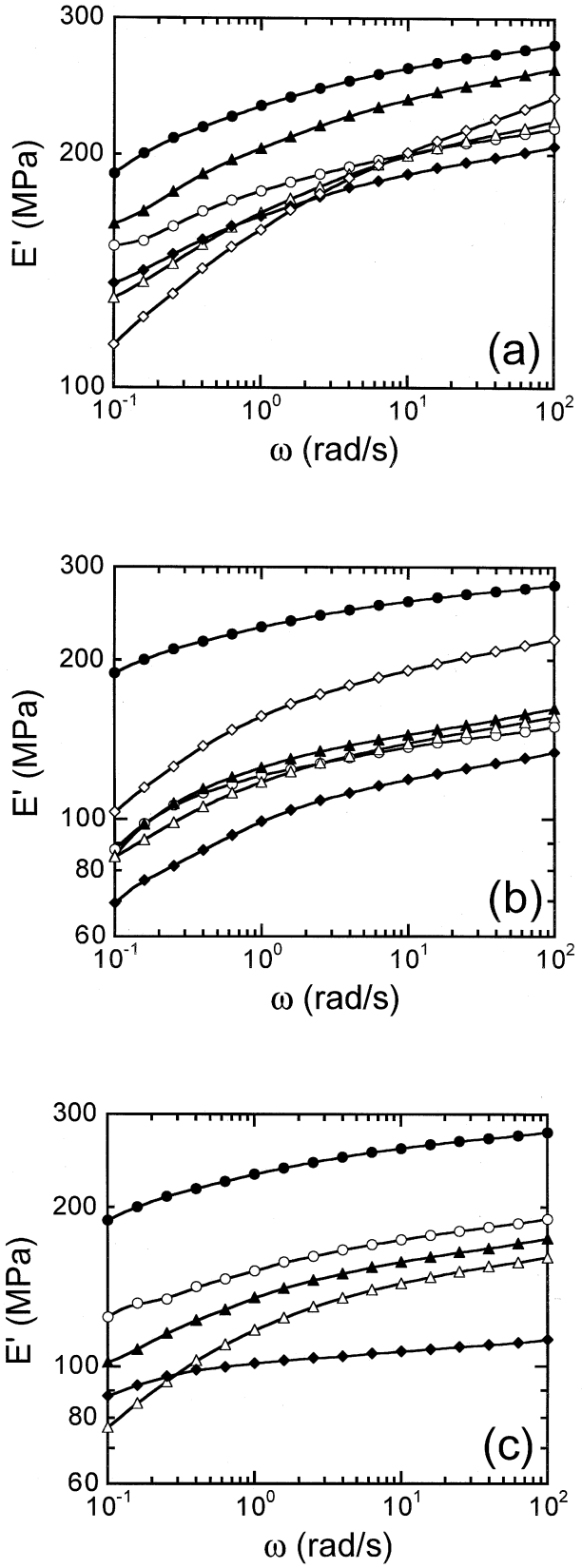

Figure 15. Dependence of E' on ω for SIS/SI blends composed of (a) SI15, (b) SI30 and (c) SI48. In each series, w_{SI} is varied: 0.0 (●), 0.2 (○), 0.4 (▲), 0.6 (△), 0.8 (♦) and 1.0 (◇). The solid lines serve to connect the data.

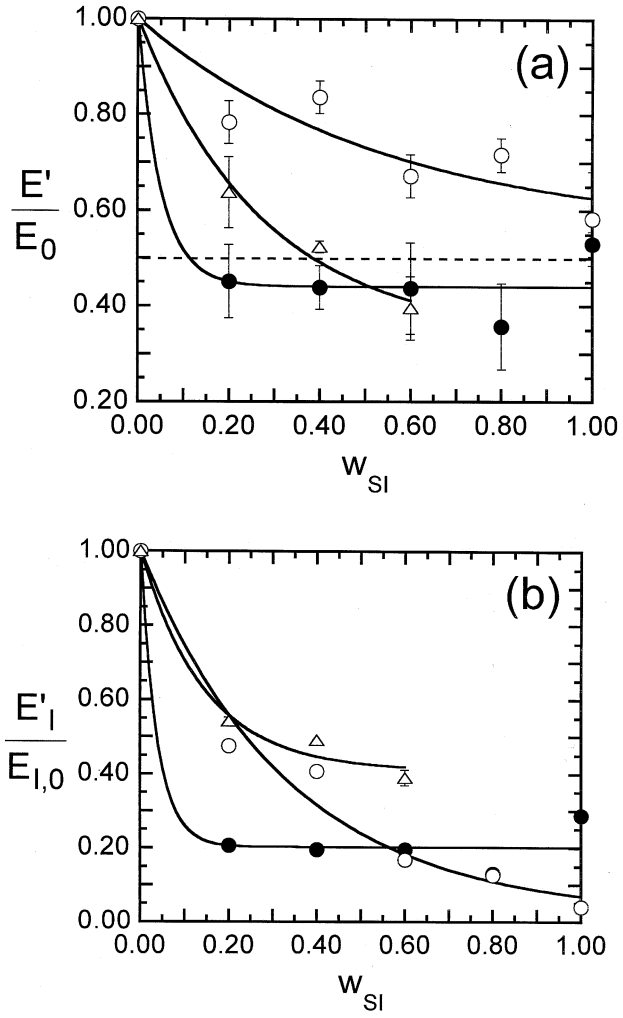

Figure 16. In (a), variation of E'/E_0 with w_{SI} for lamellar SIS/SI blends with SI15 (○), SI30 (●) and SI48 (△). Corresponding values of $E'_I/E_{I,0}$ deduced from the GM model (Equation (2) in the text) are provided as a function of w_{SI} in (b). The solid lines in both figures serve as guides for the eye, and the dashed line in (a) identifies $E'/E_0 = 0.5$.

SAXS and TEM analyses, this blend possesses a bicontinuous morphology (which has not been conclusively identified at the present time). The composition dependence of E'/E_0 is presented in Figure 16a, whereas that of $E'_I/E_{I,0}$ from the GM model (Equation (2)) is reported for comparison in Figure 16b. Both figures confirm that E'/E_0 (as well as $E'_I/E_{I,0}$) generally decreases with increasing w_{SI}, in agreement with results previously reported by McKay et al.[71] This relationship is not surprising, since tails from the SI copolymers replace the bridge-forming midblocks from the SIS copolymer as w_{SI} is increased. While the SI15 copolymer is expected to induce the least pronounced reduction in E'/E_0 (or $E'_I/E_{I,0}$) due to the molecular and microdomain considerations discussed earlier regarding segmental distributions in SIS/SI blends, addition of the SI48 copolymer to the SIS copolymer should, on the basis of similar reasoning, promote the greatest reduction in E'/E_0 (or $E'_I/E_{I,0}$). According to Figure 16, this is clearly not the case. Instead, both E'/E_0 and $E'_I/E_{I,0}$ decrease sharply at $w_{SI} = 0.2$ in the SIS/SI30 blend series and remain nearly independent of w_{SI} thereafter.

Since the segmental distributions of I from the SI30 and SIS copolymers are comparable (see Figure 12b), the I tails of the SI copolymer are expected to be similar in size to the midblock loops of the SIS copolymer. From the molecular characteristics listed in Table 1, the I block of the SI30 copolymer is slightly larger than half the midblock of the SIS copolymer, indicating that the tails in the I lamellae extend marginally farther along the lamellar normal than the midblock loops. Despite this almost negligible difference, E'/E_0 (or $E'_I/E_{I,0}$) measured from the SIS/SI30 blends should not decrease more abruptly than that measured from the SIS/SI48 blends, which consist of SI molecules with much larger I tails. It is conceivable that the I tails of the SI30 copolymer sufficiently entangle the midblocks of the SIS copolymer to thwart the formation of bridges. This scenario involves non-equilibrium conditions not considered in this work. Due to the bidisperse layering within the I lamellae (see Figure 1d and 12c), the I tails of the SI48 copolymer are similarly able to entangle more than they normally would along the lamellar midplane, resulting in a less pronounced reduction in E'/E_0 (or $E'_I/E_{I,0}$). Another possibility is that E' is sensitive to the degree of microphase segregation, increasing with an increase in the degree of segregation, for a given morphology. On the basis of this consideration, the SIS/SI30 blends may possess more bridges but a lower modulus relative to the SIS/SI48 blends because the SIS/SI30 blends contain a lower molecular weight diblock and are consequently less segregated than the SI48 blends. Further analysis of these effects – entanglement dynamics and the degree of segregation – on mechanical properties in triblock/diblock blends is required to resolve this discrepancy. While the normalized modulus data in Figure 16a and 16b are qualitatively similar, an interesting difference between these two figures is that the values of $E'_I/E_{I,0}$ for blends with SI15 and SI48 are surprisingly comparable up to $w_{SI} = 0.4$ in Figure 16b.

Molecular Characteristics

Predicted values of D/R_0 (recall that R_0 denotes the unperturbed end-to-end distance of the neat SIS copolymer) for the three SIS/SI blend series are provided as a function of blend composition (expressed in terms of the volume fraction of SI, ϕ_{SI}, which is identical to w_{SI}) in Figure 17. These predictions are in favorable agreement with the experimental results presented earlier in Figure 14, verifying that the SI30 and SI48 copolymers induce lamellar swelling, whereas the SI15 copolymer promotes lamellar

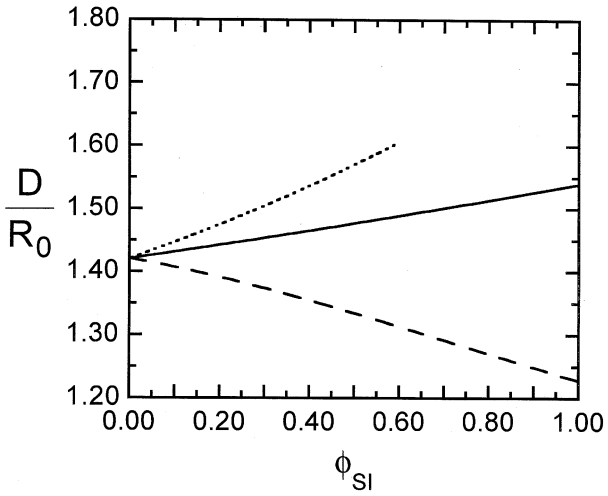

Figure 17. Predicted D/R_0 presented as a function of diblock concentration (ϕ_{SI}) for the SIS/SI blend series with SI15 (dashed line), SI30 (solid line) and SI48 (dotted line).

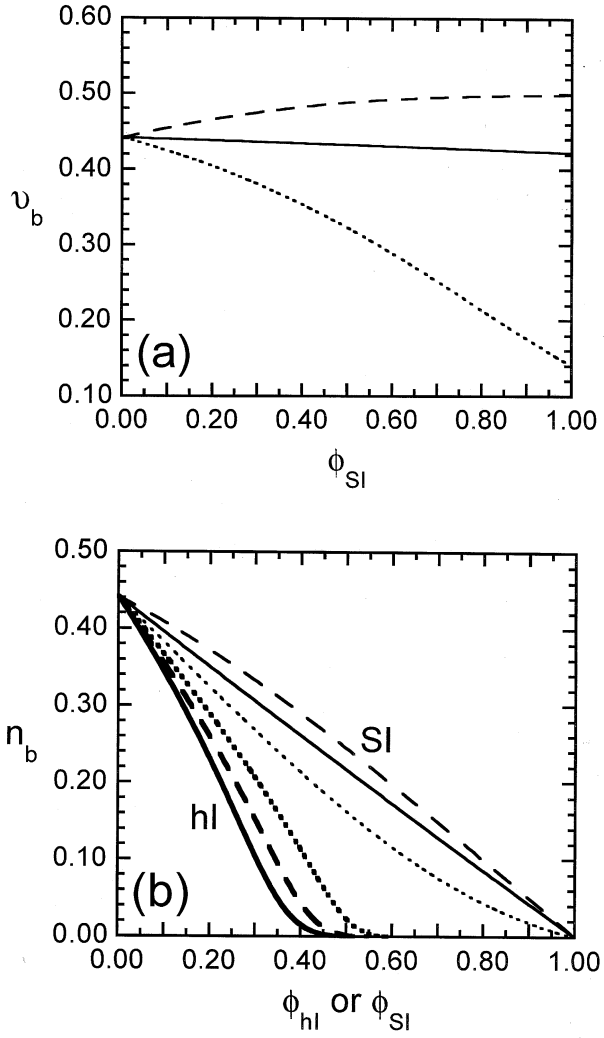

Figure 18. SCFT predictions of (a) υ_b and (b) the number of bridges per unit area of interface (n_b) as functions of blend composition (ϕ_{hI} or ϕ_{SI}) for the SIS/hI and SIS/SI blends: hI8 (dark dotted line), hI15 (dark dashed line), hI30 (dark solid line), SI15 (light dashed line), SI30 (light solid line) and SI48 (light dotted line).

shrinkage. Figure 18 shows the corresponding midblock bridge statistics for these blend series. According to the SCFT predictions presented in Figure 18a (in which υ_b is displayed as a function of ϕ_{SI}), υ_b is virtually independent of blend composition in the SIS/SI30 series, whereas υ_b decreases dramatically (from 0.44 at $\phi_{SI} = 0.0$ to 0.14 as $\phi_{SI} \rightarrow 1.0$) in the SIS/SI48 series. In marked contrast, υ_b increases with increasing ϕ_{SI} in the SIS/SI15 series due to a combination of block stratification and lamellar contraction (see Figure 1c and 12a). While these predictions provide insight into the effect of blend composition on υ_b (i.e., the number of bridged midblocks relative to the total number of midblocks present), υ_b in of itself does not solely govern the mechanical behavior of these SIS/SI blends. Recall from Figure 16 that the degree of microphase segregation may also affect the magnitude of E' in these blends. With this consideration notwithstanding, the number of connected junctions per unit area of interface (designated n_b) constitutes a more relevant measure of microdomain connectivity in triblock/diblock copolymer blends. In this case, a triblock junction is considered *connected* if its second junction resides on the adjacent interface. The magnitude of n_b, which is equal to υ_b in neat SIS copolymers, is given by $\upsilon_b(1 - \phi_{SI})$.

Predicted n_b are presented as a function of blend composition for the SIS/hI and SIS/SI blends in Figure 18b and reveal two interesting features. While n_b generally decreases non-linearly upon addition of either hI or SI, it decreases more abruptly in the presence of hI. In fact, $n_b \rightarrow 0$ at SIS/hI blend compositions near $\phi_{hI} = 0.5$. On the contrary, $n_b \rightarrow 0$ as $\phi_{SI} \rightarrow 1$ in the SIS/SI blends, indicating that bridged midblocks persist in all these blends. These predictions provide additional evidence that hI molecules are more effective at inhibiting midblock bridge formation (due to localization along the lamellar midplane) than are SI molecules (which induce intralamellar block stratification). Another important feature of Figure 18b is that the reduction in n_b at constant blend composition is more pronounced as the molecular weight of the I additive (homopolymer or copolymer block) increases due to a combination of midplane localization and an increase in lamellar width. While the SCFT predictions displayed in Figure 18b provide paradigms to be used in the design of SIS blends with specific mechanical properties, it must be remembered that they are rendered on the basis of equilibrium conditions. Non-equilibrium considerations are also expected to play an important role in the development of polymer nanostructures composed of chains/blocks differing in conformation and molecular weight, as clearly demonstrated by our results in Figure 3.

Conclusions

In this work, we have simultaneously investigated the molecular, morphological and property characteristics of triblock copolymer blends with either a midblock-selective homopolymer or a diblock copolymer. The molecular weights of the midblock-selective additives (homopolymer or copolymer block) have been systematically varied to facilitate comparison between the two blend types and elucidate the roles of molecular weight and constraint. Morphological studies of these blends by TEM and SAXS reveal that all the lamellar blends examined here are miscible and that addition of homopolymer generally induces lamellar swelling. In contrast, the lamellae in the triblock/diblock blends can be tailored to swell or contract, depending on the block lengths of the diblock copolymer. The dynamic storage modulus of the triblock/homopolymer blends decreases more abruptly relative to analogous triblock/diblock blends due to a greater reduction in the fraction of bridged midblocks, as predicted by SCFT. In some cases, the fraction of bridged midblocks in triblock/diblock blends can be increased beyond that of the neat triblock copolymer due to stratification of the constituent blocks within contracted lamellae. The results presented in this study indicate that a combined understanding of molecule-morphology-property relationships is required for the rational design of nanostructured polymer blends composed of linear multiblock copolymers.

Acknowledgement: This work was partially supported by the *Shell Development Co*. L. K. also acknowledges support from a *GAANN* Fellowship.

Received: September 5, 2000
Revised: November 13, 2000

[1] F. S. Bates, G. H. Fredrickson, *Annu. Rev. Phys. Chem.* **1990**, *41*, 525.
[2] F. S. Bates, *Science* **1991**, *251*, 898.
[3] E. L. Thomas, R. L. Lescanec, *Phil. Trans. Royal Soc. A* **1994**, *348*, 149.
[4] I. W. Hamley, "*The Physics of Block Copolymers*", Oxford University Press, New York 1998.
[5] F. S. Bates, G. H. Fredrickson, *Phys. Today* **1999**, *52*, 32.
[6] A. K. Khandpur, S. Förster, F. S. Bates, I. W. Hamley, A. J. Ryan, W. Bras, K. Almdal, K. Mortensen, *Macromolecules* **1995**, *28*, 8796.
[7] D. A. Hajduk, H. Takenouchi, M. A. Hillmyer, F. S. Bates, M. E. Vigild, K. Almdal, *Macromolecules* **1997**, *30*, 3788.
[8] M. W. Matsen, F. S. Bates, *J. Chem. Phys.* **1997**, *106*, 2436.
[9] L. A. Utracki, "*Polymer Alloys and Blends*", Hanser, Berlin 1990.
[10] C. W. Macosko, P. Guegan, A. K. Khandpur, A. Nakayama, P. Marechal, T. Inoue, *Macromolecules* **1996**, *29*, 5590.
[11] L. H. Sperling, "*Polymeric Multicomponent Materials*", Wiley, New York 1997.
[12] A. P. Smith, R. J. Spontak, H. Ade, S. D. Smith, C. C. Koch, *Adv. Mater.* **1999**, *11*, 1277.
[13] N. Furgiuele, A. H. Lebovitz, K. Khait, J. M. Torkelson, *Macromolecules* **2000**, *33*, 225.
[14] H. Tanaka, H. Hasegawa, T. Hashimoto, *Macromolecules* **1991**, *24*, 240.
[15] K. I. Winey, E. L. Thomas, L. J. Fetters, *Macromolecules* **1991**, *24*, 6182.
[16] K. I. Winey, E. L. Thomas, L. J. Fetters, *J. Chem. Phys*. **1991**, *95*, 9367.
[17] R. J. Spontak, S. D. Smith, A. Ashraf, *Macromolecules* **1993**, *26*, 956.
[18] R. G. H. Lammertink, M. A. Hempenius, E. L. Thomas, G. J. Vancso, *J. Polym. Sci., Part B: Polym. Phys.* **1999**, *37*, 1009.
[19] D. A. Hajduk, P. E. Harper, S. M. Gruner, C. C. Honeker, G. Kim, E. L. Thomas, L. J. Fetters, *Macromolecules* **1994**, *27*, 4063.
[20] M. W. Matsen, *Phys. Rev. Lett.* **1995**, *74*, 4225.
[21] M. W. Matsen, *Macromolecules* **1995**, *28*, 5765.
[22] A. D. Vilesov, G. Floudas, T. Pakula, E. Yu. Melenevskaya, T. M. Birshtein, Yu. V. Lyatskaya, *Macromol. Chem. Phys.* **1994**, *195*, 2317.
[23] J. Zhao, B. Majumdar, M. F. Schulz, F. S. Bates, K. Almdal, K. Mortensen, D. A. Hajduk, S. M. Gruner, *Macromolecules* **1996**, *29*, 1204.
[24] R. J. Spontak, J. C. Fung, M. B. Braunfeld, J. W. Sedat, D. A. Agard, L. Kane, S. D. Smith, M. M. Satkowski, A. Ashraf, D. A. Hajduk, S. M. Gruner, *Macromolecules* **1996**, *29*, 4494.
[25] T. Hashimoto, K. Yamasaki, S. Koizumi, H. Hasegawa, *Macromolecules* **1993**, *26*, 2895.
[26] L. Kane, M. M. Satkowski, S. D. Smith, R. J. Spontak, *Macromolecules* **1996**, *29*, 8862.
[27] S. Sakurai, H. Irie, H. Umeda, S. Nomura, H. H. Lee, J. K. Kim, *Macromolecules* **1998**, *31*, 336.
[28] R. J. Spontak, *Macromolecules* **1994**, *27*, 6363.
[29] M. W. Matsen, *J. Chem. Phys.* **1995**, *103*, 3268.
[30] M. W. Matsen, F. S. Bates, *Macromolecules* **1995**, *28*, 7298.
[31] S. T. Milner, T. A. Witten, M. E. Cates, *Macromolecules* **1989**, *22*, 853.
[32] S. T. Milner, *Science* **1991**, *251*, 905.
[33] S. D. Smith, R. J. Spontak, M. M. Satkowski, A. Ashraf, J. S. Lin, *Phys. Rev. B* **1993**, *47*, 14555.
[34] Y. Matsushita, Y. Mogi, H. Mukai, J. Watanabe, I. Noda, *Polymer* **1994**, *35*, 246.
[35] Y. Tselikas, N. Hadjichristidis, R. L. Lescanec, C. C. Honeker, M. Wohlgemuth, E. L. Thomas, *Macromolecules* **1996,** *29*, 3390.
[36] M. W. Matsen, *J. Chem. Phys.* **1995**, *102*, 3884.
[37] R. Stadler, C. Auschra, J. Beckmann, U. Krappe, I. Voigt-Martin, L. Leibler, *Macromolecules* **1995**, *28*, 3080.
[38] S. Brinkmann-Rengel, V. Abetz, R. Stadler, E. L. Thomas, *Kautsch. Gummi Kunstst.* **1999**, *52*, 806.
[39] J. H. Laurer, S. D. Smith, J. Samseth, K. Mortensen, R. J. Spontak, *Macromolecules* **1998**, *31*, 4975.
[40] A. M. Mayes, M. Olvera de la Cruz, *J. Chem. Phys.* **1989**, *91*, 7228.
[41] M. W. Matsen, R. B. Thompson, *J. Chem. Phys.* **1999**, *111*, 7139.
[42] M. W. Matsen, *J. Chem. Phys*. **2000**, *113*, 5539.
[43] J. H. Laurer, D. A. Hajduk, J. C. Fung, J. W. Sedat, S. D. Smith, S. M. Gruner, D. A. Agard, R. J. Spontak, *Macromolecules* **1997**, *30*, 3938.
[44] A. Avgeropoulos, B. J. Dair, N. Hadjichristidis, E. L. Thomas, *Macromolecules* **1997**, *30*, 5634.

[45] M. W. Matsen, *J. Chem. Phys.* **1998**, *108*, 785.
[46] E. B. Zhulina, A. Halperin, *Macromolecules* **1992**, *25*, 5730.
[47] M. W. Matsen M. Schick, *Macromolecules* **1994**, *27*, 187.
[48] R. L. Jones, L. Kane, R. J. Spontak, *Chem. Eng. Sci.* **1996**, *51*, 1365.
[49] B. Q. Li, E. Ruckenstein, *Macromol. Theory Simul.* **1998**, *7*, 333.
[50] H. Watanabe, *Macromolecules* **1995**, *28*, 5006.
[51] H. Watanabe, T. Sato, K. Osaki, M.-L. Yao, A. Yamagishi, *Macromolecules* **1997**, *30*, 5877.
[52] K. Karatasos, S. H. Anastasiadis, T. Pakula, H. Watanabe, *Macromolecules* **2000**, *33*, 523.
[53] D. A. Norman, L. Kane, S. A. White, S. D. Smith, R. J. Spontak, *J. Mater. Sci. Lett.* **1998**, *17*, 545.
[54] If we assume that only loops reaching the midplane of the B lamellae become interdigitated, then the population of interdigitated loops will exactly equal that of bridges. This equality occurs in the lamellar microphase, because half of the B blocks reaching the midplane will, by symmetry, form bridges. For this reason, the bridging fraction can never exceed 0.5.
[55] S. A. White, M. J. Hicks, S. R. F. McCartney, G. L. Wilkes, *J. Appl. Polym. Sci.* **1996**, *61*, 663.
[56] B. L. Riise, G. H. Fredrickson, R. G. Larson, D. S. Pearson, *Macromolecules* **1995**, *28*, 7653.
[57] S.-H. Lee, J. T. Koberstein, X. Quan, I. Gancarz, G. D. Wignall, F. C. Wilson, *Macromolecules* **1994**, *27*, 3199.
[58] T. Hashimoto, H. Tanaka, H. Hasegawa, *Macromolecules* **1990**, *23*, 4378.
[59] J. H. Laurer, S. A. Khan, R. J. Spontak, M. M. Satkowski, J. T. Grothaus, S. D. Smith, J. S. Lin, *Langmuir* **1999**, *15*, 7947.
[60] B. J. Dair, C. C. Honeker, D. B. Alward, A. Avgeropoulos, N. Hadjichristidis, L. J. Fetters, M. Capel, E. L. Thomas, *Macromolecules* **1999**, *32*, 8145.
[61] H. Watanabe, T. Sato, K. Osaki, *Macromolecules* **2000**, *33*, 2545.
[62] M. Takayanagi, K. Imada, T. Kajiyama, *J. Polym. Sci. C* **1966**, *15*, 263.
[63] I. M. Ward, D. W. Hadley, "*An Introduction to the Mechanical Properties of Solid Polymers*", Wiley, New York 1993.
[64] J. J. Aklonis, W. J. MacKnight, "*Introduction to Polymer Viscoelasticity*", Wiley, New York 1983.
[65] R. J. Albalak, E. L. Thomas, *J. Polym. Sci. B: Polym. Phys.* **1994**, *32*, 341.
[66] R. W. Gray, N. G. McCrum, *J. Polym. Sci. A-2* **1969**, *7*, 1329.
[67] T. M. Birshtein, Yu. V. Lyatskaya, E. B. Zhulina, *Polymer* **1990**, *31*, 2185.
[68] P.-Y. Lai, E. B. Zhulina, *Macromolecules* **1992**, *25*, 5201.
[69] R. Levicky, N. Koneripalli, M. Tirrell, S. K. Satija, *Macromolecules* **1998**, *31*, 2616.
[70] C. M. Papadakis, K. Mortensen, D. Posselt, *Eur. Phys. J.* **1998**, *4*, 325.
[71] K. W. McKay, W. A. Gros, C. F. Diehl, *J. Appl. Polym. Sci.* **1995**, *56*, 947.